RESEARCH



Nomadic innovation in small-scale iron acquisition inspired by and dedicated to marginal steppe environments of Mongolia

Jang-Sik Park¹ · William Gardner² · Jargalan Burentogtokh³

Received: 3 November 2022 / Accepted: 1 January 2023 / Published online: 12 January 2023 © The Author(s), under exclusive licence to Springer-Verlag GmbH Germany, part of Springer Nature 2023

Abstract

Pastoral nomadic groups in the Eurasian steppe were in existence for more than a few millennia, paving the way for the emergence of steppe polities that maintained close and dynamic interactions with their sedentary farming neighbors. Despite the critical role of iron materials in the genesis of these mobile political entities, surprisingly little is known about the mode of iron acquisition adopted by mobile pastoralist groups. This is particularly true for mobile communities located far away from the population centers where technological capabilities and material resources were more likely to converge in innovative ways. In this article, we present a microscopic examination of small cast iron objects bearing evidence of a unique thermal treatment in the molten state to obtain rapid decarburization, specifically for small-scale steelmaking from a non-local material, cast iron. This highly sophisticated technique was carried out on-site at a Mongol period habitation located in north-central Mongolia. These findings are important as they demonstrate that mobile pastoralists of the Mongolian steppe developed various methods of small-scale iron production that allowed them to enjoy a degree of self-sufficiency in one of the most critical areas of material culture, iron, and steel production.

Keywords Mongolia · Mongolian Empire · Small scale · Iron acquisition · Innovation

Introduction

Though technological innovations have a lasting impact on the history of societies, many times these changes transpire in unexpected ways that can be unrecognized for various reasons. Take, for example, the acquisition of iron and iron tools among mobile pastoralist groups of the Mongolian steppe. Long-standing tacit assumptions held that the dispersed mobile communities did not possess the technical capabilities required to supply themselves and thus relied on

William Gardner william.gardner@yale.edu

Jargalan Burentogtokh jargalanb@num.edu.mn

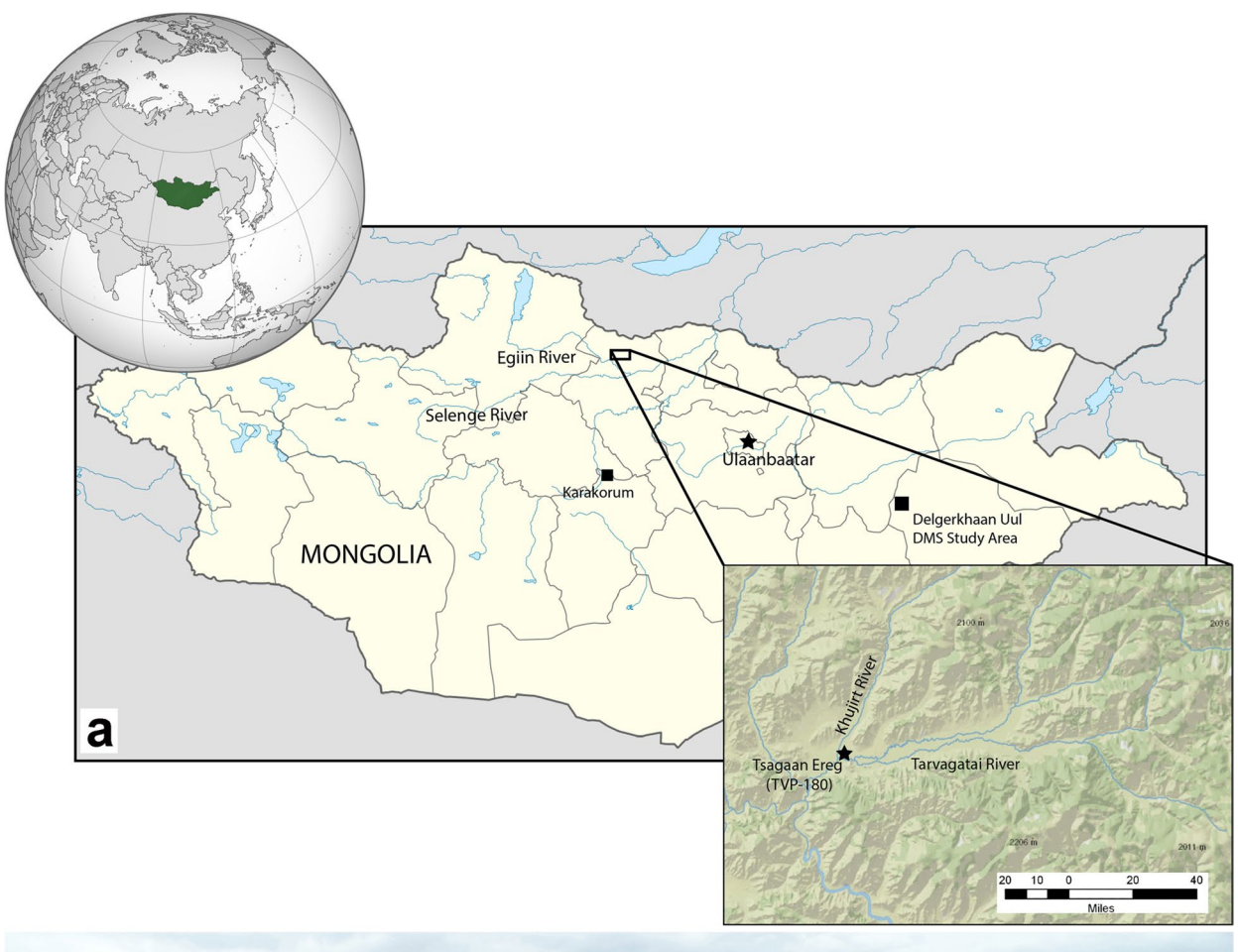
- Department of Materials Science and Engineering, Hongik University, Jochiwon 30016, Sejong, Korea
- Department of Anthropology, Yale University, New Haven, USA
- Department of Anthropology and Archaeology, National University of Mongolia, Ulaanbaatar, Mongolia

external sources for the acquisition of iron and iron objects (Khazanov 1994; Jagchid and Hyer 1979). In part, these assumptions owed to the fact that little attention was paid to nomadic iron production in general.

Recent metallographic studies of iron objects from the royal tombs of the first regional polity of the eastern steppe, the Xiongnu state (ca. 200 BC to 150 AD), have provided new perspectives (Park et al. 2010, 2018; Honeychurch 2015). These elite grave sites provide evidence for large-scale iron production that could not be fulfilled by simply relying on imports from outside sources. Even more intriguing is that most of the objects recovered were derived from bloomery-based iron technology that was a technique different from the metallurgical traditions of neighboring sedentary communities of the contemporary Han Dynasty (Rostoker and Bronson 1990; Wagner 1996, 2008). Furthermore, evidence has emerged from the analysis of iron artifacts retrieved from excavations at the Mongol Empire capital of Karakorum that suggests these steppe-derived metallurgical practices were maintained for centuries (Park and Reichert 2015).

Based on the most current research, there is little doubt that a bloomery-based iron tradition was the dominant mode of iron production practiced at major political centers in Mongolia









▼Fig. 1 Map and site photographs. a A map of Mongolia showing the location of the archaeological site Tsagaan Ereg (TVP-180) in the Tarvagatai Valley, as well as the Delgerkhaan Uul, and Karakorum sites, mentioned in the text. b An aerial photograph taken from a drone camera facing to the north toward the Khujirt River Valley

from at least the Xiongnu polity through to the Mongol Empire (Amartuvshin et al. 2012; Sasada and Ishtseren 2012; Ishtseren and Sasada 2014; Sasada and Chunag 2014). Given that these findings come from royal cemeteries and political centers, it is tempting to presume that iron production was controlled by political elites who used the distribution of this critical resource to co-opt the dispersed mobile pastoralist communities that formed their political base. Given the vastness of these mobile polities and the key strategic importance of iron, such a complete reliance on "down-the-line" support emanating from central places was unlikely. In fact, archaeological investigations in Mongolia have produced mounting evidence suggesting that the presence of community-based iron production was commonplace (Houle and Broderick 2011).

Less is known, however, about the nature of technology that allowed for small-scale iron manufacturing and especially the local production of steel. Recent metallographic work (Park et al. 2019a, 2019b) on the iron assemblages from medieval mobile pastoralist sites in the Delgerkhaan Uul area (Fig. 1a) of eastern Mongolia has produced notable discoveries. These studies recognize the scale of production as a key factor to be considered in the implementation of a specific iron technology in steppe environments. Attention has since been directed to small iron fragments, conventionally thought of as scrap metal, that would otherwise have been overlooked as something of little practical or metallurgical value.

During the summer of 2019, numerous iron objects in the form of small irregular fragments were excavated from a Mongol Period habitation site located in the Tarvagatai Valley of north-central Mongolia (see Fig. 1a). Based on the medieval archaeometallurgical analysis carried out in the east, their significance was immediately recognized, and metallographic examination was carried out to determine their intended purpose and the engineering processes applied for their production. This article presents a detailed account of the analysis, results, and a discussion of the mode of iron acquisition employed in the forest-steppe region of north-central Mongolia as compared with that at Delgerkhaan Uul, located in the arid zone of eastern Mongolia.

Comments on the Tsagaan Ereg (TVP-180) archaeological settlement

Formed by the Tarvagatai River, a tributary to the greater Egiin Gol River, the Tarvagatai Valley consists of approximately 120 km² of habitable land in the forest-steppe

region of the Baikal rift zone in north-central Mongolia. The basal elevation of the east-to-west flowing Tarvagatai River is approximately 950 msl (meters above sea level). Physical relief in the valley is created by the Buteel Mountain range to the north and east (reaching 1850 msl) and the Khantain Mountain range to the south (reaching 1650 msl). Over the last 10 years, the Tarvagatai Valley Project (TVP) has conducted an intensive pedestrian survey of over 86 km². As a result of these field efforts, multiple regions in the valley have been identified as locales preferred for habitation by both mobile pastoralists in antiquity and present-day herders. Dozens of such areas have been subjected to intensive auger testing, geophysical prospection, and small- and large-scale block excavations. For this study, we examine twenty iron and ironrelated objects recovered from the excavation of a Mongol period habitation at the Tsagaan Ereg site (TVP-180 see Fig. 1a). The Tsagaan Ereg site (TVP-180) was first identified during pedestrian survey given that large amounts of cultural material were eroding out of a cut bank incised by the Tarvagatai and Khujirt Rivers. The cultural material analyzed in this paper comes from "Dwelling #2" which was located along the edge of the cut bank created by the Tarvagatai River, as shown in Fig. 1b, an aerial photograph taken from a drone camera facing to the north toward the Khujirt River Valley. The rough extent of the dwelling was later confirmed by geophysical prospection conducted by Dr. Bryan Hanks of the University of Pittsburgh. Excavations were carried out there in the summer of 2019 by archaeologists from the Mongolian National University, Yale University, and the University of Wyoming.

Following methodological examples employed at excavations of Paleoindian dwellings (Kornfeld and Frison 2000; Stiger 2006), a premium was placed on in situ artifact identification and point-plot mapping. Specific attention was given to the recovery of highly accurate locational information for artifact types as related to soil conditions in order to distinguish disturbed versus in situ contexts for an accurate reconstruction of possible activity areas (Todd and Waguespack 2007). To further ensure tight locational integrity of excavated materials, the excavation of arbitrary 5 cm levels was conducted by trowel across an excavation block that was divided into 1-×-1-m excavation units. These excavation units were further subdivided and excavated into 50-cm-x-50-cm quadrants. By confining excavation into small compartments within the unit, the excavator's attention was purposefully focused on identifying artifacts in situ (Gardner and Burentogtokh 2018). Additionally, this method of excavation provides tighter locational control over artifacts recovered from soils sieved through a 3 mm mesh screen. In total, 11 sq. m were excavated to a depth of approximately 1.2 m below the ground surface with



excavations terminating at a sterile C soil horizon consisting of loess deposits.

Based on the radiocarbon dating of two separate bone collagen samples, the habitation structure dates to cal. AD 1290-1400. The time range of occupation is based on a bone collagen sample found in-place, embedded into the original floor of the dwelling space (F.S. 2611; UGAMS# 44,800, cal. AD 1298-1400 95.4% probability) and a second bone collagen sample in the fill material deposited after the abandonment of the dwelling (F.S. 2487: UGAMS# 46,821, cal. AD 1290–1395 95% probability). Based on our current interpretation of the archaeological remains, we believe the occupants of the dwelling space created a circular, semisubterranean habitation by excavating approximately 51 cm into the underlying loess deposit and then erecting a nonpermanent superstructure (of unknown material) that was supported by a series of wooden posts. It also appears that at some point the structure was accidentally or intentionally burned down, a birch bark floor was then laid down over the subsequent ash lens, and the structure was re-inhabited. Upon abandoning the dwelling, loess sediment (possibly fill stockpile resulting from the original construction) and surrounding cultural debris were used to fill in the living area (Burentogtokh and Adiyasuren 2019). All proceeding artifacts we discuss in this paper were mixed with the loess sediment that was used to fill in the dwelling area. Given that radiocarbon dates from both the fill material and the living surface so closely overlap, we are confident that the refuse material mixed with the fill was from the time of occupation of the dwelling space.

Lastly, during the excavation of the dwelling space, a small iron-working feature was discovered in the southeast sector of the living area (Fig. 2). This smelter consisted of two rock-lined pits located immediately adjacent



Fig. 2 A photograph showing the two furnace structures installed in the southeast sector of the living area. The scale bar 20 cm in length is broken into two 10 cm sections, one of which is a single 10 cm block with the other broken into 1 cm blocks



to one another. Both pits had an opening on their western side, and one pit held oxidized loess fill. The second pit contained small charcoal flecking, clinker, and slag materials and had two tunnels entering the pit from the south. These tunnels appear to be part of a flume that facilitated airflow. Based on the clinker, slag fill, and presence of a potential flume, it appears that this feature functioned as a small work area for smelting iron ore.

Comments on artifacts

The general appearance of the iron objects under consideration is illustrated in Fig. 3 where the actual size of each can be inferred by referring to the common scale bar located near the upper right corner. These objects, selected for examination from the numerous metal fragments excavated, represent those relatively large in size. Their weight, however, is 26.4 g or less except object #4, which weighs 52.8 g, with the majority of them being less than 10.0 g. Most of these artifacts are irregular in shape and bounded by uneven surfaces suggestive of treatments applied at high temperatures, which is further supported by the small metal piece tightly welded to the larger block at the bottom as indicated by the light arrow in objects #1 and 2.

For the benefit of later discussion, the objects in Fig. 3 were arranged according to the type of materials and treatments employed as determined by microscopic analysis, which is described in detail in the following sections. Objects derived from cast iron (#1–16) are placed ahead of those made of bloomery iron (#17-20). In objects #14, 15, and 16, the fracture surface created when they were broken off the parent article is still readily identifiable, indicating that they were given no significant thermal treatment subsequently. In contrast, the rest of the objects derived from cast iron have lost their initial shape as formed during the original casting operation. The thermal treatment given to them afterwards was certainly responsible for this deformation. The deformation is particularly prominent in objects #1-9 displaying features characteristic of a solidification reaction. In contrast, the deformation in objects #11-13 does not clearly define whether the treatment was applied in the liquid state or not. Though not clearly visible in Fig. 3, object #10 takes the form of a thin plate with its cross-section tapered as would be expected in a blade, which is a clear sign of the application of mechanical working. It is important to note that if fragments labeled #14, 15, and 16 had been treated in the molten state then they would have been deformed resulting in the loss of their current shape, as was the case for objects #1-9.

Objects #17–20 of bloomery origin were included for the sake of thoroughness with the presentation of analytical results minimized as seen in Table 1. In general,

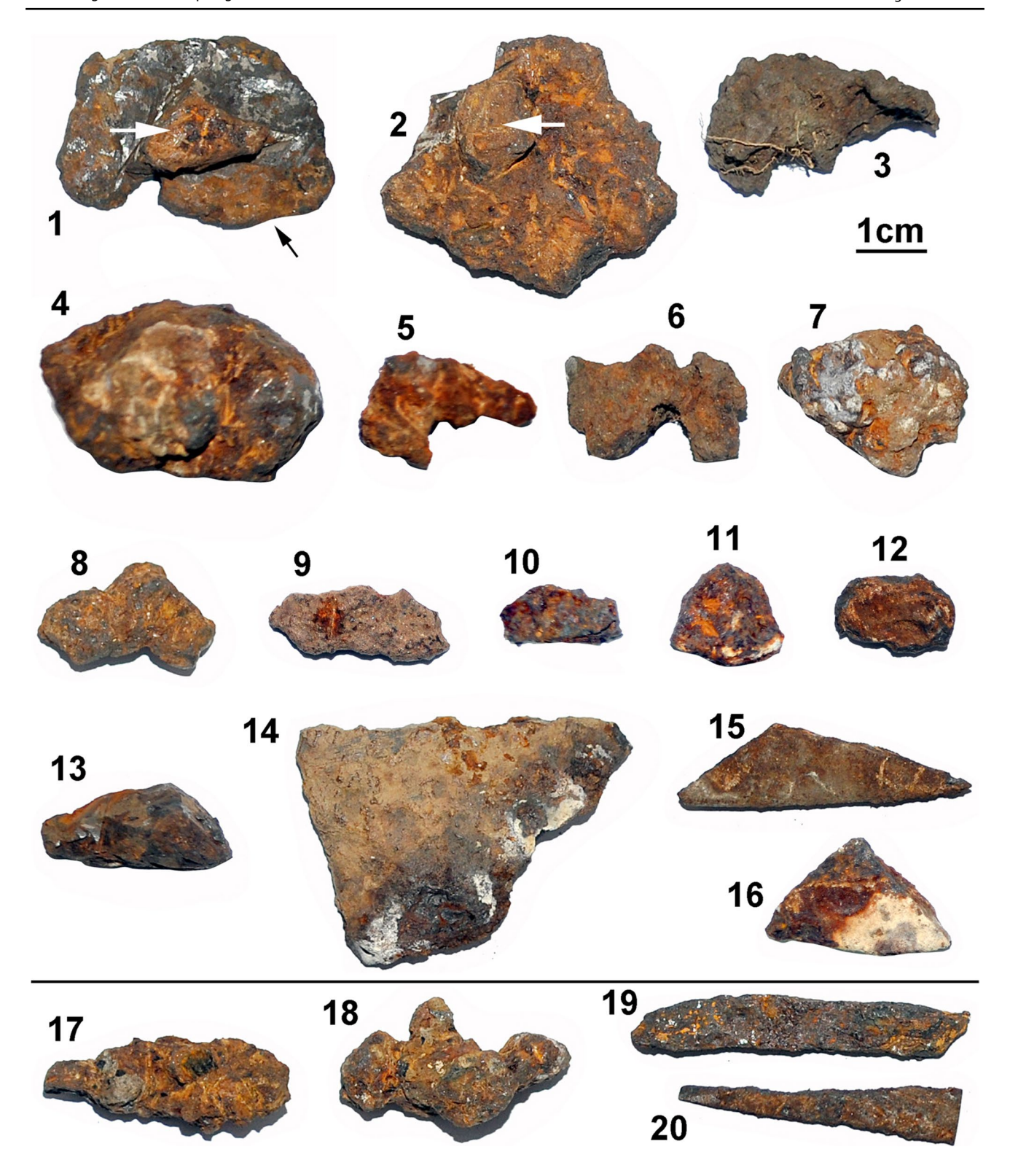


Fig. 3 The general appearance of the iron objects under consideration. Objects #1–9 are fragments with an irregular surface profile characteristic of the solidification reaction from the partially molten state; #10 a plate with the tapered cross section as in a blade; #11–13

fragments with a shape displaying no hint of a treatment given in the molten state; #14-16 fragments in as-cast states; #17-20 bloomery products. The objects are shown approximately to scale and labeled consistently with Table 1



these samples possess structures and chemical compositions qualitatively identical to those reported previously on the iron and iron-related assemblage derived from bloomery-based technology. Bloomery production was a contemporaneous technological practice evidenced at both Tasgaan Ereg and other nearby archaeological sites located within the Tarvagatai Valley (Park et al. 2020). However, bloomery production is substantially different from the technological process we identify in the objects made from cast iron scrap metal (#1–16) and discussed in detail below.

Metallographic examination

One or more specimens were taken from each of the iron objects illustrated in Fig. 3 for metallographic examination. The specimens were mounted and polished following standard metallographic procedures (Scott and Schwab 2019) and then etched using a solution of 2% nitric acid by volume in methanol, for investigation using an optical microscope and a scanning electron microscope (SEM: JEOL JSM-5410) in the secondary electron image (SEI)

mode with the accelerating voltage set at 20 kV. The microstructures observed were used to infer the carbon concentration. The presence of other minor elements such as silicon (Si), phosphorus (P), and sulfur (S) was assessed using the energy-dispersive X-ray spectrometer (EDS) included with the SEM, the nominal detection limit of which is within a few tenths of a percent. The chemical composition was specified to the nearest 0.1% according to weight fraction. The EDS instrument was calibrated using cobalt (Co) as a standard while the built-in elemental standards provided by OXFORD instruments were utilized for quantitative chemical analysis. EDS spectra were taken from the surface of etched specimens away from corroded areas.

Figure 4a presents an optical micrograph covering the entire cross-section of object #1 in Fig. 3, exposed upon sectioning along the direction indicated by the dark arrow. The smaller piece placed at the upper right corner used to be part of the specimen attached to the lower left corner of Fig. 4a, which was separated during sampling. No structural discontinuity is visible in Fig. 4a near the boundary between the small rectangular upper block and the bottom plate, indicating that they were once in the liquid state, which allowed for metal flow as illustrated in their complete welding.

Table 1 The metal fragments examined from the medieval site at Tarvagatai in north-central Mongolia and their Field ID, mass, and chemical composition. The numbers labeling the objects are consistent with those in Fig. 3

#	ID	Treat	Find Spot #	Depth (cm)	Mass (g)	Composition (wt. %)				Comments
						C	Si	P	S	
Cas	t iron products		'							
1	44-P10#1	^a R	2242	80	20.0	1.0	0.8	0.5	0.9	2 pieces welded
2	38-P6#2	R	2318	86.8	26.4	1.3	0.7	0.4	0.9	2 pieces welded
3	33-P5#1	R	399	19.3	13.0	1.3	0.9	0.7	1.3	
4	47-P12#5	R	2091	80.3	52.8	1.3	0.8	0.4	0.8	
5	57b-P7#2	R	2552	95	9.8	1.3	0.3	0.4	0.8	
6	23-P3#1	R	740	25	6.5	1.3	0.3	0.3	0.6	
7	27-P3#9	R	2784	26.1	17.6	1.0-3.5	0.0 – 0.2	0.0	0.0	
8	43-P9#1	R	2576	104	5.2	1.5-3.5	0.0 – 0.2	0.4-0.6	0.5-0.9; 1.6	
9	55-P5#9	R	1369	16.7	2.5	0.8 - 1.0	0.6	0.0	0.0	
10	54a-P4#2	R-bF	2415	97	1.6	0.8	0.2	0.0	0.2	Spherical ^c CM, blade
11	57a-P7#2	R	2554	95	0.9	1.5	1.1	0.4	0.6	Flake ^d Gr
12	62d-P17#1	eHT	1902	73.4	1.4	1.3	0.5	0.6	2.1	Shapes display no hint of re-melting
13	34-P5#2	As-cast	313	16.7	10.7	2.5	0.5	0.3	0.7	
14	50-P19#1	As-cast	1859	66.7	25.9	1.0	0.4	0.3	2.1	
15	49-P18#3	As-cast	1823	65	7.8	2.5	0.8	0.4	1.8	
16	62b-P15#2	As-cast	1303	51.2	7.3	2.8	1.1	0.5	1.2	
Blo	omery products	S								
17	30P4#4	^f NA	2383	93.4	8.0	< 0.02	${}^{\mathrm{g}}\mathrm{ND}$	0.3	ND	Only ferrite
18	42P8#1	NA	2466	97.6	10.1	0.0 – 0.8	ND	ND	ND	Ferrite and pearlite
19	40P7#1	NA	2535	99	8.3	0.1 - 0.8	ND	ND	ND	Ferrite and pearlite
20	48P13#1	NA	905	36.7	2.5	0.0 - 0.5	ND	ND	ND	Ferrite and pearlite

^aR, remelted; ^bF, forged; ^cCM, cementite; ^dGr, graphite; ^eHT, heat-treated in the solid state; ^fNA, not applicable; ^gND, none detected



The structure is remarkably uniform over the entire cross-section except in a few limited areas. Figure 4b, an optical micrograph taken at arrow 1 in Fig. 4a, provides a magnified view of the structure dominating the specimen, which consists of numerous dark particles of a roughly spherical shape with their boundaries being outlined by the bright layer. Figure 4c is a SEM micrograph covering roughly the same area as Fig. 4b, which is another attempt to visualize these spherical particles. The particles represent pearlite, and their boundaries are filled with cementite or white cast iron eutectic. It should be noted that the pearlite areas used to be occupied by proeutectic austenite, which was subsequently transformed into the current structure.

Such a unique spherical structure emerges when cast iron is treated at a temperature above the liquidus threshold (Park et al. 2019b). Under an oxidizing atmosphere, this treatment would cause decarburization to take place, allowing the molten cast iron to solidify at a relatively uniform temperature. In this case, the solidification reaction is not driven by heat flow but by the gradual reduction of general carbon concentration in the molten alloy, leading to the nucleation and growth of the primary austenite phase in the form of spheres rather than in dendritic forms. Given these conditions, the growth of primary austenite would continue until the process is terminated. The structure in Fig. 4b and c represents a case where the solidification reaction was nearly completed by the precipitation of proeutectic austenite, which subsequently transformed to pearlite. Further treatment would have had no molten alloys left at their boundaries to be precipitated in the form of eutectic, making it difficult to infer how the structure developed. The carbon concentration may then be determined at around 1.0%, given the structure in Fig. 4b and c consisting primarily of pearlite particles of 0.77% carbon content with a little cementite-rich space at their boundaries. This value, though an approximation based on microstructure, is sufficient for discussion in this study.

Figure 4d, an optical micrograph enlarging the area at arrow 2 in Fig. 4a, shows dark particles, similar to those in Fig. 4b in size and shape, sparsely scattered over the eutectic background. The carbon concentration in this area is therefore a little less than 4.3% of the eutectic composition, a value much higher than the overall carbon level of the specimen determined at approximately 1.0%. The bright area evidently remained in a liquid state at the termination of the process when the rest of the specimen was nearing the end of the solidification reaction and was mostly filled with spherical proeutectic austenite. The fine eutectic structure as compared with the coarse proeutectic particles in Fig. 4d is an unmistakable sign of the remaining liquid solidifying rapidly during the subsequent cooling stage.

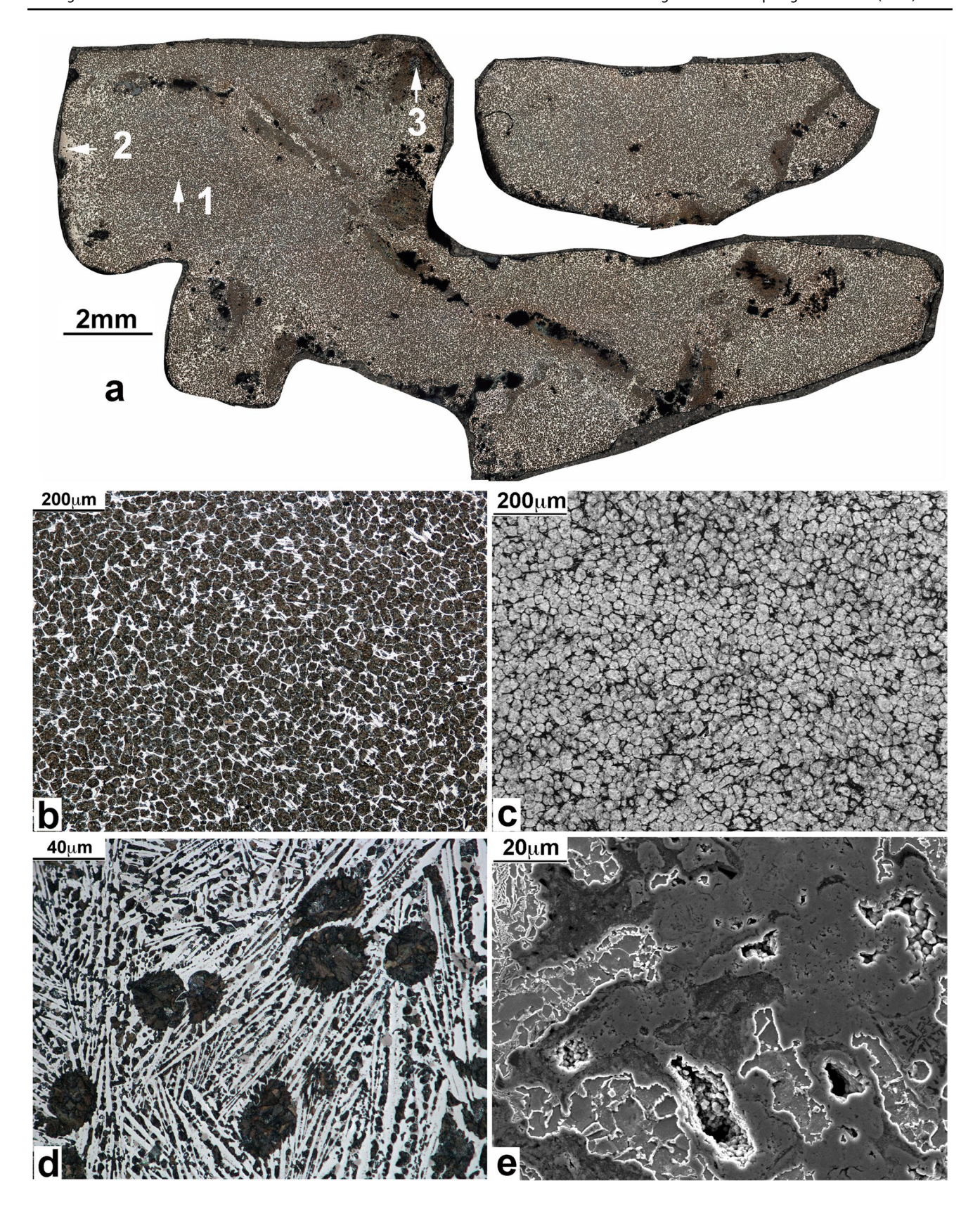
The opposite cases are confirmed in the areas appearing darker than their neighborhood, one of which is located at arrow 3 in Fig. 4a. Microscopic examination at higher

magnification reveals that they also consist of numerous spherical pearlite particles such as those seen in Fig. 4b. Their boundaries in these areas, however, were much reduced and barely visible. In these areas, the solidification reaction during the controlled thermal treatment must have significantly reduced the molten alloy available for the following uncontrolled solidification. On the other hand, Fig. 4e, a highly magnified SEM micrograph taken at arrow 3 of Fig. 4a, illustrates the presence of an unusual structure at the center of this dark pearlite area. In Fig. 4e, bright ferrite grains are preferentially positioned at the left and bottom edges, indicating that this particular metal part was completely decarburized. EDS analysis shows that the rest of the micrograph was filled with a material made primarily of iron oxide. This oxygen-bearing ingredient likely served as an agent indispensable for the promotion of such accelerated and complete decarburization.

Microstructures virtually identical to those illustrated in Fig. 4a were also observed in objects #2–6 of Fig. 3. Objects #7-11 had clear signs of a similar thermal treatment applied. The structural development, however, was not the same. Figure 5, covering the cross-section of object #7, is seen to consist of multiple regions of varying carbon concentration, reflected in distinctly different microstructures. The vicinity of arrow 1 shows dark particles spread over a bright background of white cast iron eutectic. These particles take a roughly spherical shape just like those in Fig. 4b and d. Some of them, however, take the form of dendrites, which is indicative of slightly non-uniform temperature distribution set along their growth direction. Regardless of their exact shape, the dark areas represent the proeutectic area precipitated out of the liquid in a thermal treatment similar to that discussed above. The significant fraction of eutectic is indicative of an earlier termination of the process. The neighborhood of arrow 2, however, had no eutectic precipitated, suggesting that the solidification reaction was completed by the growth of the proeutectic phase even before the process was terminated. That such a structural difference was observed in the above two areas, only a few millimeters apart, evidently reflects the steep gradient in oxygen potential established in the reaction atmosphere, which plays a key role in determining the rate of decarburization.

Figure 6a, a SEM micrograph from object #10 in Fig. 3, displays the cementite phase precipitated mostly in the form of fine particles, with some exceptions located in the pearlite regions. Such a peculiar structure allows the average carbon level to be determined near the eutectoid, 0.77%, and is indicative of the thermal treatment applied near the eutectoid temperature, 727 °C. This treatment, which transforms the lamellar cementite in pearlite into a spherical form, is frequently accompanied by mechanical working as a means to enhance the transformation rate, which seems to have been the case with object #10, given that it assumes the shape of







▼Fig. 4 Optical and SEM micrographs taken from the specimen of object #1 in Fig. 3. a Optical micrograph covering the entire cross-section cut along the direction indicated by the dark arrow in object #1 of Fig. 3; the small piece presented at the upper right corner was broken off the bottom left part of the specimen. b Optical micrograph magnifying the area at arrow 1 in Fig. 4a. c SEM micrograph covering approximately the same area as Fig. 4b. d and e Optical and SEM micrographs enlarging the spots marked by arrows 2 and 3 in Fig. 4a, respectively

a thin plate. Spherical cementite, particularly in high-carbon steel, is preferred as it improves fracture resistance upon impact loading. It is important to note that the two large particles indicated by the arrows in Fig. 6a represent iron sulfide. Such sulfide particles serve as a distinctive sign of cast iron smelted in a mineral coal-fired reaction environment (Park 2015; Park et al. 2019c). Those in Fig. 6a, therefore, confirm coal-smelted cast iron employed as the raw material for the given object. Their presence was identified in most cast iron-derived objects under consideration. No such particle, however, was found in the bloomery objects presented in Fig. 3.

Figure 6b, a SEM micrograph from object #11 in Fig. 3, shows that the graphite phase precipitated in the form of dark curved flakes. These are preferentially located at the boundaries between proeutectic particles such as those observed in Fig. 4c. The object must therefore have been given a similar treatment as discussed above. Upon its termination, however, the remaining molten alloy was apparently solidified to form gray cast iron eutectic, which consists of graphite and austenite. In this specimen, the silicon level as inferred from EDS analysis was particularly high and determined at around 1.1%. Such high silicon content was evidently responsible for the precipitation of gray cast iron eutectic (Park 1990).

Figure 6c, an optical micrograph showing the structure of object #14 in Fig. 3, consists largely of coarse pearlite forming the background with some cementite particles located in the bright areas, some of which are marked by the arrows labeled A. The average carbon content as inferred from this structure is approximately 1.0%. Object #14 is a fragment broken off a cast iron article. The fracture surface, which is still visible, suggests no thermal treatment was applied after the breakage. An iron-carbon alloy with such a low carbon level is not desirable for casting because of its high melting point and inferior flow properties. As such, the parent article of object #14 was likely cast from an alloy of much higher carbon content and then treated for decarburization to improve its impact resistance. This treatment in the solid state was apparently successful in reducing the carbon content. However, the numerous sulfide particles remaining in the specimen, as shown in the arrows labeled B in Fig. 6c, suggest that the treatment was not effective at lowering the specimen's sulfur level (see Table 1). Given the detrimental effect of sulfide inclusions on the material properties of steel, the possibility of reducing their density could be another advantage that is frequently overlooked in the discussion of the treatment applied to molten cast iron.

Finally, Fig. 6d, an optical micrograph taken of the specimen from object #16 of Fig. 3, illustrates the presence of numerous proeutectic dendrites with the space between them filled with cementite or white cast iron eutectic. This structure is typical of those emerging in the solidification of cast iron alloys whose carbon level is set significantly below 4.3%. No sign is visible in Fig. 6d of a significant thermal treatment applied after the casting operation, which is in agreement with what is suggested by the object's external appearance. The given object, if treated in the molten state, would undergo a similar transformation in its appearance with its carbon concentration reduced to the range of steel.

The carbon concentration of the specimens examined, and their silicon, phosphorus, and sulfur contents are presented in Table 1 along with brief information about artifact ID, treatments applied, and mass. The numbers labeling the objects in Table 1 are consistent with those in Fig. 3, where objects #1–16 are derived from cast iron while objects #17-20 are of bloomery origin. Microscopic and visual examination confirms that objects #1-11 were treated in the molten state. Their carbon concentration mostly falls within the narrow range of 0.8 to 1.5%, with some exceptional cases where evidence of non-uniform and incomplete treatments was observed. It should be noted that objects #12-14, without being treated in the molten state, had their carbon level reduced to 1.0–1.3%, suggesting a treatment applied in the solid state. Objects #15 and 16 with their carbon content set at 2.5 and 3.0%, respectively, may be representative of those items available in fragmentary form as cast iron feed materials for further treatments.

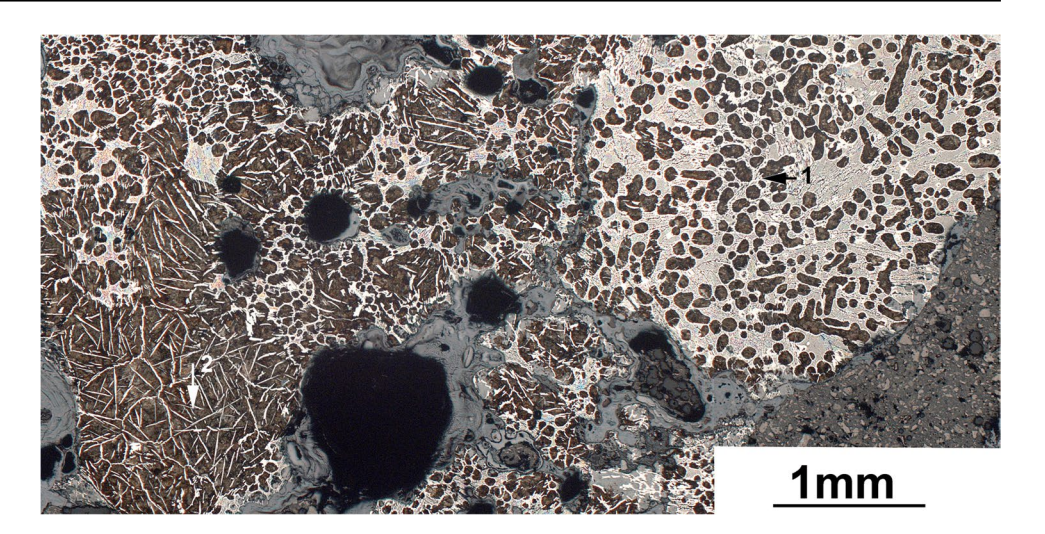
Discussion

A thermal treatment involving cast iron in the molten state, apparently for decarburization, was evident in the external appearance of the objects under consideration. A visual inspection could therefore readily distinguish between those with (objects #1–9 in Fig. 3) and without (objects #15–16) treatment. The latter represent fragments broken off from parent cast iron articles and, in their present form, have little practical value. If treated for decarburization, however, they could be readily transformed into steel, an invaluable material for making highly functional items. The assemblage shown in Fig. 3, therefore, consists of closely associated metal objects as an input and an output material for an engineering process intended for making steel from cast iron.

The unique microstructure consisting of numerous spherical particles of pearlite with their boundaries filled with



Fig. 5 Optical micrograph illustrating the structure observed in object #7 of Fig. 3



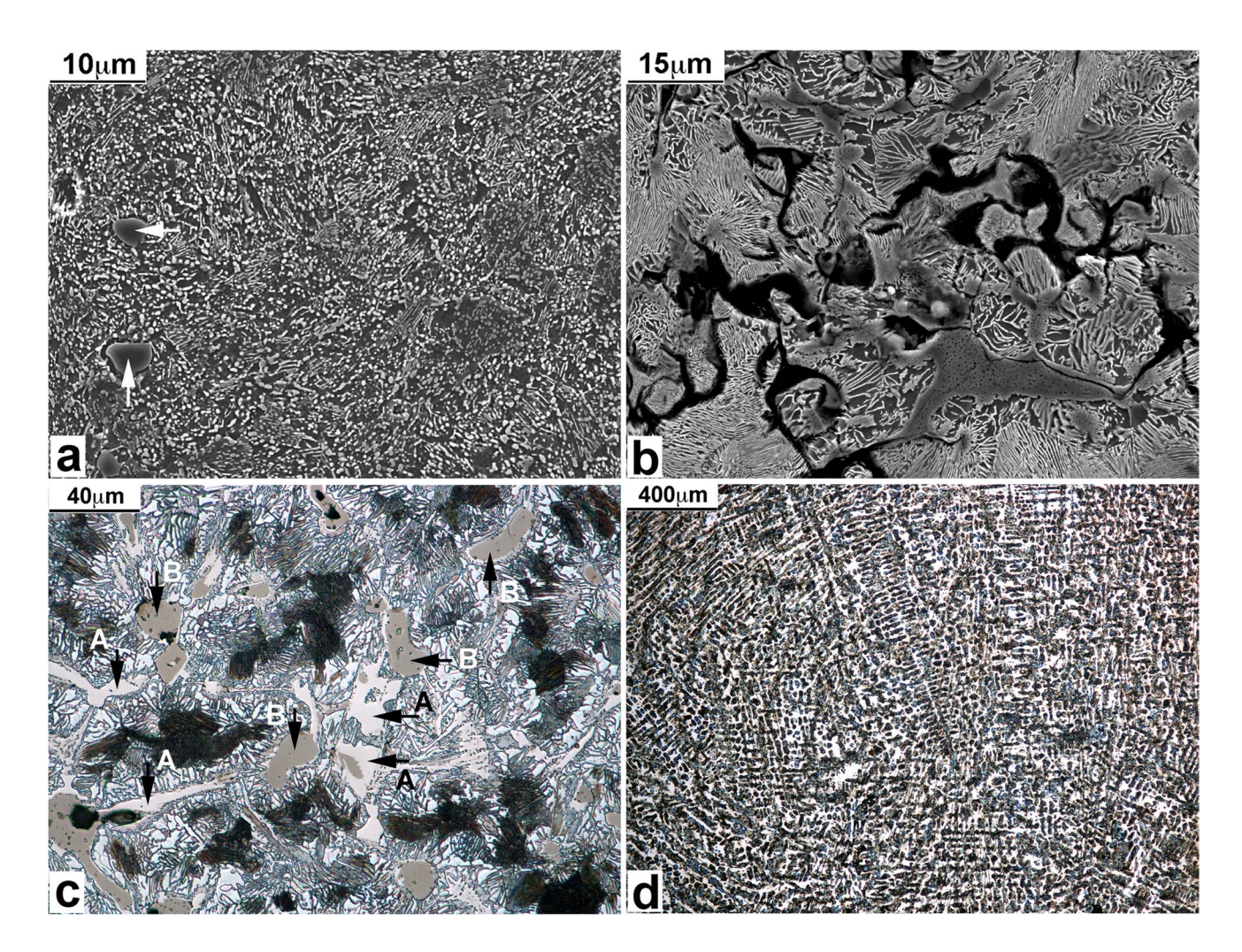


Fig. 6 Optical and SEM micrographs (a). b SEM micrographs showing the structure of objects #10 and 11 in Fig. 3, respectively. \mathbf{c} and \mathbf{d} Optical micrographs showing the structure of objects #14 and 16 in Fig. 3, respectively



white cast iron eutectic graphically illustrates the phase transition occurring in cast iron when treated in the molten state for decarburization (Park et al. 2019b). In this treatment, the decreasing carbon level in the molten alloy drives the nucleation and growth of the proeutectic phase in spherical forms. If the treatment is terminated prematurely, the remaining liquid solidifies during the subsequent cooling stage to precipitate eutectic at the boundaries. As such, the fraction of eutectic in specimens thus treated may vary significantly from zero to a hundred percent. This variability was in fact confirmed in some of the samples examined including objects #7–10. The structures observed in objects #1-6, however, were remarkably uniform and consistent, suggesting the existence of a technological guideline, though rudimentary, circulating as a reference for the process. The average carbon concentration inferred from these structures ranges from 1.0 to 1.3% as listed in Table 1, which was likely the target composition intended. This carbon level is well within the range of steel.

The major advantage of steel over cast iron is that it can accept substantial plastic deformation without being broken. In certain circumstances, this valuable property justifies the investment required for such a small-scale decarburization process by which small pieces of metal can be individually treated. Object #10 provides an example of those items decarburized and then forged into a usable form, in this case, a thin plate. Given the additional loss of carbon during the forging operation (Park 2008), its current carbon level of approximately 0.8% allows the original carbon concentration to be assessed at around 1.0–1.3%. This estimation agrees with what is inferred from objects #1-6, which were given a successful thermal treatment and were ready to be forged. By virtue of this technique, object #10 has enough carbon to ensure strength while its cementite phase precipitated in the form of spherical particles (see Fig. 6a) offers improved toughness. The tapered cross-section of the object suggests that it was in the process of being made into a microblade, weighing only 1.4 g.

By the time of the Mongol Empire, when the objects in Fig. 3 were produced, steelmaking by treating molten cast iron had long been practiced in the neighboring sedentary farming societies of eastern Asia. This technique, however, was employed primarily at an industrial scale and could not be applied to such a small-scale production effort as reflected in the assemblage of Fig. 3. In any case, the reduction of carbon concentration from 3.0 to 1.3%, as inferred from the data in Table 1, requires the reaction temperature to be controlled within a relatively narrow range at around 1300 °C. This temperature control can only be achieved in a covered environment providing thermal insulation. A proper means to supply oxygen is also necessary whether for combusting fuels or for controlling the reaction atmosphere. The exact nature of the process and the infrastructure employed has yet to be documented in Mongolia. Considering the furnace features discovered at the Tsagaan Ereg settlement (Fig. 2), it is important to note that these were likely used for bloomery smelting and are too large to support the steelmaking operation discussed here (Park et al. 2020). However, the presence of these furnaces does indicate the practical knowledge and technological capacity required to carry out such metallurgical processes.

The equipment needed to implement steel making from individually treated cast iron fragments, weighing mostly 10.0 g or less, would not have been very large or complex. A small container, more like a crucible, with a means for supplying necessary oxygen would have sufficed. The irregular shape of most objects in Fig. 3 also demonstrates that they were treated on a flat surface with nothing else to guide the shape formation during solidification. The reaction temperature therefore must have been set to have the molten metal confined by its own surface tension force. If the diffusion coefficient of carbon along the liquidus of the iron-carbon system is taken to be 10^{-4} cm²/s (Verhoeven 1975: 154), the distance of carbon diffusion for a hundred seconds is determined at approximately 1.0 mm. This distance is much larger than the microstructural scale observed in the treated samples (see Fig. 4b). With the proper control of reaction temperature and atmosphere, therefore, it may have taken a few minutes for most objects in Fig. 3 to have their carbon level reduced to the target range.

According to our typological and radiocarbon periodization of sites with such steelmaking remains across the two regions, most objects were recovered from Mongolian Empire contexts (thirteenth-fourteenth centuries AD) with some exceptions dating to the prior Khitan period (tenth-twelfth centuries AD). This chronological estimation is in line with the extremely high level of sulfur detected in most iron objects since it was derived from the use of mineral coal in smelting, which commenced in Mongolia during the Khitan period and was carried forward into the period of the Mongol Empire (Park et al. 2008, 2015, 2019c). The successful implementation of this metallurgical process would not have been possible without a comprehensive understanding of the physical properties of iron-carbon alloys as determined by the various thermo-mechanical treatments applied. Moreover, the technique would not have been innovated if not appropriate for the needs and capabilities of daily life on the steppe. The fact that it was routinely practiced in several regions like the Tarvagatai Valley of northern Mongolia as well as at Delgerkhaan Uul, 700 km to the southeast, underscores the uniformly high level of technological sophistication attained by mobile pastoralists (Park et al. 2019a). Evidently, the pertinent technological methods were widely shared by pastoralist groups across the expansive Mongolian steppe.

Because this small-scale process was scaled to the needs of local herding communities, it is not the kind of technology expected to be employed in major central places, such as the imperial capital city of Karakorum. The technique, therefore,

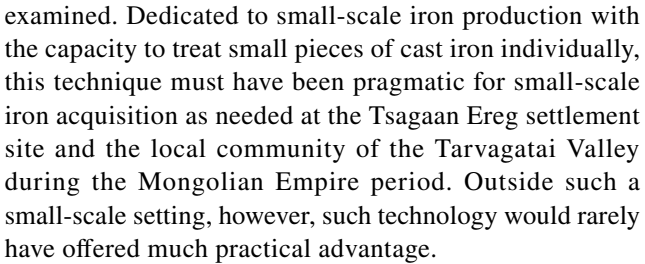


was probably not borrowed from such central places or from surrounding sedentary neighbors but was developed indigenously within these outlying herding communities. However, cast iron in scrap form was a necessary input for this steelmaking operation, and during this period, cast iron would have been a product of urban centers with large-scale, specialized metallurgical industries. As such, this particular mode of iron acquisition would have required connections to major population centers with a capacity to produce and accumulate cast iron, and such access would have depended on the skills of local pastoralist groups to network within a setting of regional and inter-regional politics. Such a cast iron-based technology, therefore, points to local ironworking as a practice necessarily engaged with regional steppe political arenas, particularly for the acquisition of non-local raw materials.

This premise accords well with the assessed periodization of the Tsagaan Ereg site, which was inhabited during the Mongolian Empire when steppe groups throughout the eastern steppe territory were under imperial administration. The Mongol Empire also notably integrated much of Eurasia into multiple large resource distribution networks (Erdenebat et al. 2022), and these long-distance exchange capabilities were also important for making cast iron from China widely available to steppe nomads in the north. It is important to remember, however, that indigenous bloomery-based technology was still in practice as a significant alternative for iron acquisition, indicating that iron production was achieved through two fundamentally different methods. Local pastoralists, who likely practiced semi-specialized production, relied either on cast iron-based or bloomery iron-based technology or, as in the case of the Tsagaan Ereg settlement, employed both methods simultaneously. This unique dual technological tradition probably allowed local herding groups substantial freedom and flexibility in securing the strategic materials of iron and steel that they required, without relying too closely on external political networks which, as politics want to do, varied in dependability.

Conclusion

Of the numerous iron fragments recovered from the Tsagaan Ereg medieval habitation site in the Tarvagatai Valley of north-central Mongolia, a group of metal objects was subjected to visual and microscopic investigation. Most of them were small pieces less than 20.0 g in weight with irregular shapes and surface features characteristic of applied thermal treatments. Metallographic examination found this assemblage to consist primarily of metal fragments derived from cast iron with some notable exceptions of bloomery origin. Microstructures illustrating a thermal process practiced for making steel from molten cast iron were observed in many of those specimens



This unique technique evidently played a key role in the emergence of a technological tradition based on both modified cast iron and bloomery iron. The important role of cast iron as noted above suggests that pastoralist groups in the steppe had ready access to various supply chains to be provided with this non-local material. Even with such a heavy reliance on cast iron, however, indigenous bloomery ironbased technology was still in practice. Such a dual mode of iron production, offering more options and flexibility, would have allowed most local groups to remain self-sufficient with less external support necessary. The consistent microscopic data presented above alluded to an important fact that this steelmaking process was routinely practiced at such a small scale as to be run by a few workers who were not full-time specialists dedicated to metalworking; i.e., they were most likely metallurgical semi-specialists who also herded animals and held other local responsibilities. This capacity would have greatly expanded the number of local communities that could manage this technological process in order to fulfill their own need.

Key aspects of the Mongol medieval period may have stimulated the establishment of such a cast iron-dependent ironworking tradition. These likely included factors ranging from political conditions, such as state-backed efforts to maintain extensive interaction networks (Honeychurch and Amartuvshin 2006), to technological factors including an overall increase in the consumption of cast iron (Park and Reichert 2015) and use of mineral coal-based smelting (Park et al. 2008; Park 2015). Though not mentioned in the historical sources, imperial authorities may have recognized the advantage of such an independent ironworking tradition and likely encouraged and perhaps even sponsored its implementation. This individual mode of iron acquisition could have been instrumental for Mongol cavalry soldiers of the early imperial period who were expected to be a self-supplied force without depending on a central authority for the provision of mounts, weapons, and armor (Atwood 2004: 350). A similar technique practiced contemporaneously in eastern Mongolia (Park et al. 2019a) suggests that communities across the vast Mongolian steppe region were well connected and coordinated under uniform technological and political settings, ready to be mobilized.

Given its importance for small-scale and independent iron acquisition combined with the long history of cast iron use



and availability in Mongolia (Park et al. 2007, 2018), this unique steelmaking technology was likely conceived much earlier and reserved as an alternative production method with its advantages fully acknowledged. Given the inevitable reliance on non-local cast iron, its implementation was most likely determined by regional and inter-regional politics and social settings. The Mongol period certainly fostered one of the best environments for the full potential of this technology to be exploited. It is important to note, however, that the metal assemblage from Karakorum, one of the many prominent political centers of the Mongol empire, has provided no convincing evidence of a similar technique having been practiced there (Park and Reichert 2015). Indeed, the technique under consideration was a nomadic innovation inspired by and dedicated to local steppe communities that would have supported an emphasis on flexibility as part of a long-standing cultural and social tradition on the eastern steppe (Honeychurch 2014). The dual technologies reflected in the metallurgical assemblages observed in the Tarvagatai Valley and at Delgerkhaan Uul are precisely the kind of small-scale and diversified practices that would enhance productive options and alternatives for the needs of local nomadic communities. We anticipate that continued research on the extent to which this technique was implemented in conjunction with bloomery-based ironworking will provide further insight into the flexible nature of nomadic organization and complexity in ancient Mongolia.

Acknowledgements This work would not have been possible without the generous collaboration of the Institute of Archaeology, Mongolian Academy of Sciences. Special thanks are due to Ms. Adiyasuren Molor for her helpful assistance in securing the samples for analysis. Dr. William Honeychurch at Yale University is greatly appreciated for his insightful suggestions on interpreting the analytical results from an archaeological perspective. The analytical work was conducted while the author (JSP) was a professor at Hongik University.

Author contribution JSP: conceptualization, data analysis, investigation, methodology, funding acquisition, writing—original draft and preparation. WG: fieldwork, resources, funding acquisition, writing—review and editing. JB: fieldwork, resources, funding acquisition, writing—review and editing.

Funding The fieldwork, analyses, and research presented here were financially supported by grants from the National Research Foundation of Korea (NRF-2017R1A2B4002082) and the National Science Foundation of the USA (NSF-1737687 and 1822559).

Data availability Not applicable.

Code availability Not applicable.

Declarations

Competing interests The authors declare no competing interests.

Ethics approval Not applicable.

Consent to participate Not applicable.

Consent for publication Not applicable.

Conflict of interest The authors declare no competing interests.

References

- Amartuvshin Ch, Sasada T, Eregzen G, Usuki I, Isheren L (2012) Khustyn Bulagiin dursgalt gazart ilersen tomoriin khuder khailuulakh bolon vaar shataakh zuukhny on tsagiin asuudald. Arkheologiin Sudlal 32:213–228
- Atwood C (2004) Encyclopedia of Mongolia and the Mongol Empire. Facts on File, New York
- Burentogtokh J, Adiyasuren M (2019) Archaeological and paleoclimatic research in Tarvagatai Valley of Teshig sum in Bulgan aimag, 2019. Report on file with the Mongolian Academy of Science's Institute of Archaeology, Ulaanbaatar, Mongolia
- Erdenebat U, Burentogtokh J, Honeychurch W (2022) The archaeology of the Mongol Empire. In: May T, Hope M (eds) The Mongol World. Routledge Publications, London, pp 507–533
- Gardner WRM, Burentogtokh J (2018) Mobile domiciles of the Eurasian steppe: archaeological evidence of possible dwelling space during the early Iron Age. J Field Archaeol 43(5):345–361
- Honeychurch W (2014) Alternative complexities: the archaeology of pastoral nomadic states. J Archaeol Res 22:277–326
- Honeychurch W (2015) Inner Asia and the spatial politics of empire: archaeology, mobility, and culture contact. Springer Publications, New York
- Honeychurch W, Amartuvshin Ch (2006) States on horseback: the rise of inner Asian confederations and empires. In: Stark M (ed) Archaeology of Asia. Blackwell, Malden, MA, pp 255–278
- Houle J-L, Broderick L (2011) Settlement patterns and domestic economy of the Xiongnu in Khanui Valley, Mongolia. In: Brosseder U, Miller B (eds) Xiongnu archaeology: multidisciplinary perspectives of the first steppe empire in Inner Asia. Rheinische Friedrich-Wilhelms- Universität, Bonn, pp 137–152
- Ishtseren L, Sasada T (2014) Khunnugiin toriin khuder khailuulakh zuukhny sudalgaany zarim asuudal. Arkheologiin Sudlal 34:253–263
- Jagchid S, Hyer P (1979) Mongolia's culture and society. Westview Press, Boulder CO
- Khazanov A (1994) Nomads and the outside world. University of Wisconsin Press, Madison
- Kornfeld M, Frison GC (2000) Paleoindian occupation of the high country: the case of middle park. Colorado Plains Anthropologist 45(172):129–153
- Park JS (2008) The key role of forging in ancient steelmaking from cast iron. Mater Charact 59:647–650
- Park JS (2015) The implication of varying 14C concentrations in carbon samples extracted from Mongolian iron objects of the Mongol period. J Archaeol Sci 63:59–64
- Park JS, Chunag A, Gelegdorj E (2008) A technological transition in Mongolia evident in microstructure, chemical composition and radiocarbon age of cast iron artifacts. J Archaeol Sci 35:2465–2470
- Park JS, Erdenebaatar D, Eregzen G (2018) The implication of the metallurgical traditions associated with Chinese style wagons from the royal Xiongnu tomb at Golmod 2 in Mongolia. Archaeol Anthropol Sci 10:1535–1546. https://doi.org/10.1007/s12520-017-0476-7
- Park JS, Eregzen G, Yeruul-Erdene Ch (2010) Technological traditions inferred from iron artefacts of the Xiongnu Empire in Mongolia. J Archaeol Sci 37:2689–2697
- Park JS, Gardner WRM, Burentogtokh J (2020) Micro-scale iron smelting in early Iron Age to Mongol Period Steppe communities of



- North-Central Mongolia and its implications. Asian Archaeol 3:75–82. https://doi.org/10.1007/s41826-020-00031-5
- Park JS, Honeychurch W, Chunag A (2019) Iron technology and medieval nomadic communities of eastern Mongolia. Archaeol Anthropol Sci 11:555–565. https://doi.org/10.1007/s12520-017-0553-y
- Park JS, Honeychurch W, Chunag A (2019) Novel micro-scale steelmaking from molten cast iron practiced in medieval nomadic communities of east Mongolia. Archaeometry 61(1):83–98. https://doi.org/10.1111/arcm.12413
- Park JS, Honeychurch W, Chunag A (2019) The technological and chronological implication of 14C concentrations in carbon samples extracted from Mongolian cast iron artifacts. Radiocarbon 61(3):831–843. https://doi.org/10.1017/RDC.2019.4
- Park JS, Reichert S (2015) Technological tradition of the Mongol Empire as inferred from bloomery and cast iron objects excavated in Karakorum. J Archaeol Sci 53:49–60
- Park JS (1990) Microstructural evolution and control in the directional solidification of Fe-C-Si alloys. Ph.D dissertation, Iowa State University, Ames, Iowa.
- Rostoker W, Bronson B (1990) Pre-industrial Iron: its technology and ethnology. In: Archaeomaterials Monograph, vol. 1. University Museum Publications, Philadelphia Pennsylvania
- Sasada T, Chunag A (2014) Iron smelting in the nomadic empire of Xiongnu in Ancient Mongolia. ISIJ Int 54(5):1017–1023
- Sasada T, Ishtseren L (2012) Chingis Khaany Ikh Ord "Avargyn balgas" daxi tomorlog uildverleliin asuudald. Arkheologiin Sudlal 32:268–277
- Scott DA, Schwab R (2019) Metallography in archaeology and art (cultural heritage science). Springer, Switzerland

- Stiger M (2006) A folsom structure in the Colorado mountains. Am Antiq 71(2):321-351
- Todd S, Waguespack N (2007) Folsom hearth-centered use of space at Barger Gulch, locality B. In: Robert H, Brunswig BL, Pitblado ? (eds) Frontiers in Colorado Paleoindian Archaeology: from the Dent Site to the Rocky Mountains. University Press of Colorado, Boulder, CO, pp. 219–260
- Verhoeven JD (1975) Fundamentals of physical metallurgy. John Wiley & Sons, New York-Chichester-Brisbane-Toronto-Singapore
- Wagner DB (1996) Iron and steel in ancient China. E.J. Brill, Leiden·New York·Köln
- Wagner DB (2008) Part 11: ferrous metallurgy. In: Needham J (ed) Science and civilization in China, Volume 5 Chemistry and chemical technology. Cambridge University Press, Cambridge

Publisher's note Springer Nature remains neutral with regard to jurisdictional claims in published maps and institutional affiliations.

Comments on providing geographical coordinates The reporting of the coordinates of the sites mentioned in the text is not possible as it violates the policies enforced by the Institute of Archaeology and the National University of Mongolia as a way to reduce looting.

Springer Nature or its licensor (e.g. a society or other partner) holds exclusive rights to this article under a publishing agreement with the author(s) or other rightsholder(s); author self-archiving of the accepted manuscript version of this article is solely governed by the terms of such publishing agreement and applicable law.

